Naval Research Laboratory

Stennis Space Center, MS 39529-5004

NRL/MR/7320--09-9176

Use of the Oregon State University Tidal Inversion Software (OTIS) to Generate Improved Tidal Prediction in the East-Asian Seas

PAUL J. MARTIN
SCOTT R. SMITH
PAMELA G. POSEY
GRETCHEN M. DAWSON
SHELLEY H. RIEDLINGER

Ocean Dynamics and Prediction Branch
Oceanography Division

March 20, 2009

REPORT DOCUMENTATION PAGE

Form Approved
OMB No. 0704-0188

1. REPORT DATE *(DD-MM-YYYY)*	2. REPORT TYPE	3. DATES COVERED *(From - To)*
20-03-2009	Memorandum Report	

4. TITLE AND SUBTITLE

Use of the Oregon State University Tidal Inversion Software (OTIS) to Generate Improved Tidal Prediction in the East-Asian Seas

5a. CONTRACT NUMBER

5b. GRANT NUMBER

5c. PROGRAM ELEMENT NUMBER
0603207N

6. AUTHOR(S)

Paul J. Martin, Scott R. Smith, Pamela G. Posey,
Gretchen M. Dawson, and Shelley H. Riedlinger

5d. PROJECT NUMBER

5e. TASK NUMBER

5f. WORK UNIT NUMBER
73-5097-B9-5

7. PERFORMING ORGANIZATION NAME(S) AND ADDRESS(ES)

Naval Research Laboratory
Oceanography Division
Stennis Space Center, MS 39529-5004

8. PERFORMING ORGANIZATION REPORT NUMBER

NRL/MR/7320--09-9176

9. SPONSORING / MONITORING AGENCY NAME(S) AND ADDRESS(ES)

Space & Naval Warfare Systems Command
2451 Crystal Drive
Arlington, VA 22245-5200

10. SPONSOR / MONITOR'S ACRONYM(S)

SPAWAR

11. SPONSOR / MONITOR'S REPORT NUMBER(S)

12. DISTRIBUTION / AVAILABILITY STATEMENT

Approved for public release; distribution is unlimited.

13. SUPPLEMENTARY NOTES

14. ABSTRACT

The Oregon State University (OSU) Tidal Inversion Software (OTIS) is being automated, tested, and used to generate tidal solutions in the East-Asian Seas (EAS) region. This effort was undertaken to improve the tidal solutions within a relocatable version of the Navy Coastal Ocean Model (NCOM). Tests were conducted within the EAS and within a smaller domain within the EAS, the Yellow Sea, to look at the effects on OTIS of a number of inputs including: (1) increasing grid resolution, (2) using more accurate bathymetry, (3) assimilating International Hydrographic Office (IHO) tide station data (as well as tidal data derived from the TOPEX altimeter data), (4) increasing the number of representers used for data assimilation, and (5) increasing the number of tidal constituents being solved for. The tidal solutions generated with OTIS were validated against IHO tide station data in the different areas.

15. SUBJECT TERMS

Tides	East-Asian Seas	4D-VAR assimilation
OTIS	Ocean modeling	Satellite altimetry

16. SECURITY CLASSIFICATION OF:			17. LIMITATION OF ABSTRACT	18. NUMBER OF PAGES	19a. NAME OF RESPONSIBLE PERSON
a. REPORT	b. ABSTRACT	c. THIS PAGE			Pamela Posey
Unclassified	Unclassified	Unclassified	UL	32	19b. TELEPHONE NUMBER *(include area code)* (228) 688-5596

CONTENTS

USE OF THE OREGON STATE UNIVERSITY TIDAL INVERSION SOFTWARE (OTIS) TO GENERATE IMPROVED TIDAL PREDICTIONS IN THE EAST-ASIAN SEAS

1. INTRODUCTION

Tides are an important part of the variability of sea-surface height (SSH) and currents in coastal and shallow-water areas and are an important component of coastal ocean models. Hence, most coastal ocean models include tides. The Naval Research Laboratory (NRL) East-Asian Seas (EAS) model (Riedlinger et al., 2006), which covers a relatively large domain (Fig. 1), has recently been modified to include tides (Riedlinger et al., 2006).

Running tides within the NRL EAS model involves two types of tidal forcing: (1) tidal potential forcing (TPF) within the interior of the model domain, and (2) tidal boundary conditions (TBCs) at the open boundaries of the domain. TPF is composed mainly of the force on the oceans due to the gravitational pull of the sun and the moon (Pond and Pickard, 1989), which is the force that drives the ocean tides. This forcing is described by fairly simple analytical functions (Webb, 1974). Note that, for a domain covering the entire earth, TBCs would not be needed, as there would be no open boundaries. In this case, the tides would be forced only by the TPF.

However, for a regional ocean domain, TBCs are needed at the open boundaries. These boundary conditions (BCs) consist of the changes in SSH and ocean currents due to the tides. The relative importance of TPF and TBCs depends on the size of the domain and its location. TPF is more important for large, deep domains that contain a large amount of water for the TPF to act upon. TBCs are relatively more important for small, shallow domains. For very small coastal domains, the TPF is frequently ignored. Even for moderately large domains, e.g., the Adriatic Sea,, which is relatively shallow over most of its area, TPF has only a small effect on the tides (Martin et al., 2006). However, for domains the size of the EAS, both TPF and TBCs are necessary.

The numerical BCs used by NRL's regional ocean models require data for both the tidal SSH and tidal currents at the open boundaries. Many early tidal databases (TDBs) included data for the tidal SSH but not the tidal currents, which significantly limits the use of these databases in ocean models. TDBs that include currents became available with the release of global and regional TDBs by Oregon State University (OSU) (Egbert et al., 2003). These TDBs made including tides in coastal and regional ocean models much easier.

OSU has made available a global and a number of regional TDBs. These have a grid resolution of 1/4° for the global TDB and 1/12° for most of the regional TDBs. The TDBs were created using the OSU Tidal Inversion Software (OTIS), which assimilates tidal data derived from satellite

Manuscript approved February 10, 2009.

altimetry within a tidal model using four-dimensional variational analysis 4D-VAR (Egbert et al., 2003).

However, as useful as the OSU TDBs are, they have some limitations, the main one being that they are frequently not very accurate in coastal areas. This is due to several factors: (1) the coarseness of the grid resolution used in generating the TDBs, (2) inaccuracies in the bathymetry used, and (3) the assimilation solely of tidal data derived from satellite altimeter measurements.

OSU has made the OTIS code freely available in order to allow researchers to derive their own TDBs. At NRL, we have been working with the OTIS package under the 6.4 Small-Scale-Prediction Project with the overall task of producing a tidal-prediction system to provide TBCs for NCOM. To accomplish this task, OTIS is being simplified, automated, and transitioned to operate within the framework of the Relocatable (RELO) NCOM system. In other words, instead of extracting and interpolating tides from a larger and coarser database, the RELO NCOM system will be able to automatically run the modified OTIS package and compute the tides at the same resolution as the specified NCOM domain. This should result in more accurate tides within the RELO NCOM domain.

Since the RELO NCOM system will most likely be run operationally in shallow marginal seas and littoral regions, accurate and high-resolution TBCs will be critical. Running OTIS at higher resolutions for these types of regions has been demonstrated to significantly improve the estimation of tides. As shown in figure 2, Egbert and Erofeeva (2002) compare a high-resolution OTIS tidal solution computed for the Indonesia Sea with the OSU global TDB. For the deep parts of this domain (depth $>$ 4000 m), the improvement was only moderate, i.e., the root-mean-square (RMS) error was reduced from 2.3 to 1.3 cm. However, for the shallower parts of the domain (depth $<$ 500 m), the improvement in accuracy was very large, i.e., the RMS error was reduced from 11.2 to 3.8 cm.

OTIS has been evolving for a number of years. OTIS was initially developed in 1994 by Gary Egbert at OSU (Egbert et al., 1994) and has since gone through several revisions and upgrades (Egbert, 1997; Egbert and Ray, 2001; Egbert and Erofeeva, 2002; Egbert and Ray, 2003; Erofeeva et al., 2003). Despite OTIS's longevity and relative robustness, the system is fairly cumbersome and complicated to use. OTIS contains a significant number of options and parameters that need to be specified by the user. For some of these options, an understanding of 4D-VAR assimilation is needed to properly set them. In order to automate the OTIS software, numerous experiments were performed to determine the options, parameters, and databases that should be used. The results of these experiments also revealed that there were several parameters that had optimal values that varied with the type of region and the resolution used. Therefore, parts of the OTIS code had to be modified or new code added to automatically compute optimal values of these parameters.

This report provides an overview of the OTIS package and some of the modifications that have been made. It also includes a summary of the results from the numerous experiments that were performed within the EAS, including marginal seas like the Yellow Sea (YS), and an analysis and comparison of the results of applying the OTIS tides to the TBCs of NCOM.

The main reasons why the EAS region was selected as the testbed for most of our experiments to date are: (1) the EAS region is strategically important to Naval operations, (2) the EAS region

is well known for containing large-amplitude tides, and 3) we have direct access to the NCOM EAS ocean forecast system, which is being run in-house at NRL.

Several different strategies were investigated to improve the tidal solutions generated for the EAS region using OTIS. These include use of (1) higher grid resolution, (2) better bathymetry, (3) additional tidal data for assimilation, and (4) inclusion of additional tidal constituents.

The sections that follow include description and/or discussion of: (1) the OSU TDBs, (2) OTIS and the procedure for running OTIS, (3) evaluation of computed tides and the evaluation grid, (4) setting up a tidal computation grid, (5) calculation of tides in the Yellow Sea with OTIS, (6) calculation of tides in the EAS with OTIS, (7) the effect of the new EAS TDBs on tides in NRL's EAS model, and (8) summary, conclusions, and future work.

2. OSU TIDAL DATABASES

OSU has generated and made available a global TDB and a number of regional TDBs, which can be downloaded from OSU's OTIS web site. Table 1 lists some of these TDBs along with the resolution at which they were generated and the tidal constituents that they include. The global TDB is at 1/4° resolution and most of the regional TDBs are at 1/12° resolution. The global TDB contains 10 tidal constituents; some of the regional TDBs contain 8 and some only the 4 (generally) largest constituents.

The first six TDBs listed in Table 1 are those that have been downloaded to date from the OSU web site for use in ocean modeling work at NRL. The other TDBs in the table are available from OSU but are not currently being used at NRL. There are other regional TDBs available from OSU that are not listed in Table 1. For the most part, these other TDBs are contained within the OTIS regional TDBs that are being used at NRL and have the same (1/12°) or similar resolution.

As noted in the introduction, there are some limitations of these TDBs that affect their accuracy and usefulness. One limitation is resolution. The use of 1/12° resolution (about 8 km) in most of the regional TDBs does not resolve the spatial variation of the tide in many coastal areas.

Another limitation is bathymetry. Although OTIS relies heavily on data assimilation, the propagation of the tides within the OTIS tidal model still depends strongly on the bathymetry. The tidal solution in shallow coastal areas, where there may not be much data to assimilate, also depends heavily on the bathymetry used. Typical available bathymetry databases do not provide accurate bathymetry for many coastal areas of the world's oceans. NRL has put a large effort into developing bathymetry databases for its ocean modeling work (see website http://www7320.nrlssc.navy.mil/DBDB2_WWW/). These NRL databases generally provide better bathymetry than those used to generate the OSU TDBs.

The OSU TDBs were generated using assimilation only of tidal SSH data derived from the TOPEX satellite altimeter. This provides good resolution of the tides in the open ocean where the spatial scale of the tides tends to be large, but not in coastal areas where the tidal spatial scale tends to be smaller and tidal variations tend to be larger.

An extensive source of tidal SSH data in coastal areas is available from the tide-station database of the International Hydrographic Office (IHO). This database consists of tidal SSH data from over

4500 tide-gauge stations scattered about the coastal areas of the world's oceans. A drawback of using the IHO data for assimilation in OTIS is that some of the stations are located within bays and estuaries where the tide is not representative of the tide in the adjacent coastal ocean, i.e., there can be significant changes in the amplitude and phase of the tide as it propagates into a bay or estuary. However, in spite of this problem, the IHO stations are a very valuable source of tidal data for the coastal ocean. It would be useful to have a characterization of the degree of "representativeness" of each IHO station for the tide in the adjacent ocean, however, we are not aware if this has ever been done and such a characterization would depend on the particular tidal constituent. Since OTIS was designed to be able to assimilate data such as that from IHO stations as well as that derived from satellite altimeters, the tidal solutions generated by OTIS can usually be improved by including assimilation of IHO data.

The OSU global TDB contains ten tidal constituents: K1, O1, P1, Q1, K2, M2, N2, S2, Mm, and Mf. Some of the OSU regional TDBs contain 8 constituents: K1, O1, P1, Q1, K2, M2, N2, and S2; however, some of the regional TDBs include only the four (generally) largest constituents: K1, O1, M2, and S2. The accuracy of the overall tide in regional ocean models should be improved by including a larger number of constituents in the high-resolution, regional tidal solutions.

Another issue is the continuity of the tides. For example, none of the OSU regional TDBs cover the entire EAS region. The OSU Yellow Sea (YS) TDB covers the Yellow Sea and part of the South and East China Seas, and the OSU Indonesia TDB covers most of the southern part of the EAS. One could take tidal data from the highest-resolution TDB available at a particular location; however, such a data set will tend to have discontinuities at the boundaries between the TDBs used. It has been found that such discontinuities can adversely affect the accuracy of the tides in an ocean model that obtains its TBCs from different TDBs.

This brings up a practical problem that is encountered in running OTIS. The computer memory and cpu time required increase greatly as the number of grid points, the size of the domain, and the amount of data to be assimilated are increased. A single TDB for the entire globe has not been generated at high resolution because the computer resources required are prohibitive. Even for a region the size of the EAS, the grid resolution and number of data values that can be assimilated are usually limited by available computational resources.

3. OTIS

3.1 OTIS description

OTIS is an assimilation tool that uses 4-D variational assimilation to assimilate SSH and velocity observations into a solution of the barotropic, shallow-water equations for a specified domain. OTIS consists of three fundamental components: the data, the ocean dynamics, and the assimilation tools to optimally combine the data and dynamics. In this section, each of these three components will be described separately.

With regard to data, OTIS has the capability of assimilating data from a wide variety of sources, including satellite altimetry, tide gauges, current meters, Coastal Ocean Dynamics Application Radar (CODAR), and Acoustic Doppler Current Profilers (ADCPs). In this implementation, however, only SSH data from satellite altimetry and tide gauges are used. This is primarily because

these two databases are global, therefore simplifying the overall use of OTIS within a relocatable system.

Since domains are almost always under-sampled, the OTIS assimilation method includes ocean dynamics to propagate information from the data locations to the entire domain. In other words, the assimilation method determines the optimal tidal solution for the entire domain that satisfies the tidal dynamics and simultaneously provides the best overall fit to the assimilated observations. To describe the dynamics of the tides, OTIS uses the linearized shallow-water equations:

$$\frac{\partial U}{\partial t} - fV + gH\frac{\partial(\zeta - \zeta_{SAL})}{\partial x} + \kappa U = \mathbf{f}_U, \tag{1}$$

$$\frac{\partial V}{\partial t} - fU + gH\frac{\partial(\zeta - \zeta_{SAL})}{\partial y} + \kappa V = \mathbf{f}_V, \tag{2}$$

$$\frac{\partial \zeta}{\partial t} = -\left(\frac{\partial U}{\partial x}, +\frac{\partial V}{\partial y}\right), \tag{3}$$

where U and V are the two components of the barotropic transport (i.e., the depth-averaged velocity times the depth H), f is the Coriolis parameter, t is the time, x and y are the distance in the two horizontal coordinate directions, g is the acceleration of gravity, ζ is the SSH, and ζ_{SAL} represents the tidal loading and self-attraction. The last term on the left-hand side of the first two equations is the linearized bottom drag (κ is a dissipation coefficient) and the terms on the right-hand side represent the earth's body tide.

OTIS has the capability of using nonlinear dynamics, which include advection and nonlinear bottom drag, but comparisons with the use of the linearized equations has shown that the inclusion of nonlinear physics significantly increases the computation cost and the resulting accuracy is only marginally, if at all, better (see Table 2). The linearized OTIS dynamics can easily be transformed from the time domain into the frequency domain using Fourier Transforms. With a little manipulation, the equations above can be expressed with the following time-independent equations:

$$\nabla \cdot gH\Omega^{-1}\nabla\zeta - i\omega\zeta = \nabla \cdot \Omega^{-1}\mathbf{f}_U - \mathbf{f}_\zeta, \tag{4}$$

$$\mathbf{U} = -gH\Omega^{-1}\nabla\zeta + \Omega^{-1}\mathbf{f}_U, \tag{5}$$

where $\Omega = \begin{bmatrix} i\omega + \kappa & -f \\ f & i\omega + \kappa \end{bmatrix}$ and $\mathbf{U} = \begin{bmatrix} U \\ V \end{bmatrix}$. When OTIS solves the forward shallow-water equations, equation 4 is used in conjunction with open boundary conditions from an OTIS TDB and depths from a bathymetry database to calculate the phase and amplitude of the SSH (ζ) at each grid point. With the SSH known, the momentum equation (Equation 5) can then be used to determine the phase and amplitude of both transport components (U and V) at each grid point.

The assimilation method used within OTIS to combine data with ocean dynamics to produce an optimal solution is called the reduced-basis representer method (Egbert et al., 1994). This method is a tool for solving variational assimilation problems that are expressed in terms of a cost function,

$$J[\mathbf{u}] = (\mathbf{Lu} - \mathbf{d})^T \sum\nolimits_e^{-1} (\mathbf{Lu} - \mathbf{d}) + (\mathbf{Su} - \mathbf{f}_0)^T \sum\nolimits_f^{-1} (\mathbf{Su} - \mathbf{f}_0), \quad (6)$$

where $\mathbf{u}$ is the state, $\mathbf{L}$ is a measurement functional that maps variables from data space to state space, $\mathbf{d}$ is the data, $\sum_e^{-1}$ is the measurement error covariance, $\mathbf{S}$ is the ocean model, $\mathbf{f}_0$ is the forcing to the model, and $\sum_f^{-1}$ is the model error covariance. The above cost function consists of two main terms, the error to the data (1st term) and the error to the model (2nd term), and the goal is to determine the optimal state $\mathbf{u}$ that minimizes the cost function J. The reduced-basis representer method is a technique for performing this minimization, in which representers are calculated for a subset of data locations and a solution to the variational problem is sought within the space of linear combinations of calculated representers.

A representer is a function showing the impact that a single observation will have on the entire domain, and is computed by first performing the adjoint of the model (the transpose of the model, $\mathbf{S}^T$) forced by a measurement functional L_k. This adjoint solution is convolved by the model error covariance ($\sum_f$) and then used to force the forward model ($\mathbf{S}$). In order to compute an exact inverse solution, the representer method would require the computation of a representer function for every individual observation. This procedure can potentially be very computationally expensive given that the TOPEX altimetry data are sampled at 1-second intervals. Therefore, instead of computing representers for all of the IHO and TOPEX data, a subset of representer locations are strategically selected and used to compute an approximate inverse solution (hence, the name "reduced-basis representer method").

In this implementation of OTIS, a total number of representers is initially determined based on available computer resources and the size of the domain. Then representers are automatically computed at all of the IHO tide-gauge locations and all of the TOPEX crossover locations. This is because these data are typically more accurate; therefore, it is desired that they have more influence within the assimilation. After the IHO stations and the TOPEX crossover points are selected, the remaining representers are strategically distributed along the TOPEX groundtracks within the domain based upon the inverse of the water depth, i.e., the shallower regions get a higher concentration of representers.

When using the reduced-basis approach, the basic assumption is that representers are similar to the representers at nearby measurement locations. Experiments have shown that the approximate inverse solution resulting from this reduced-basis approach is very close to the exact inverse solution. Therefore, when the computation time that is required to calculate the representers is factored in, the savings of using the reduced-basis approach generally far outweigh the (usually small) loss of accuracy.

3.2 Running OTIS

Our standard benchmark EAS OTIS run uses a domain extending from -17.5 to 53°N and 97.5 to 159°E, with 700 x 507 grid points, and solves for four tidal constituents. This run takes approximately 26 hours to run using a LINUX workstation (a dual-core, Advanced Micro Devices (AMD), 2.4 gHz Opteron with 16 GB of RAM).

A typical runstream script is outlined below:

1) run the set-up program to define the domain to be run, set up the grid and the bathymetry,

define the tidal constituents to be used, define the IHO data to be used for assimilation, and set up the BCs for running the forward model; run

/bin/otis_setup.x

2) set up altimetry representer and data lists; run

lat_lon -M1000

3) make the OTIS programs for the local domain, which are hard-wired for the grid dimensions and tidal constituents selected; therefore, this make needs to be redone every time a new region is set up; run

make all

4) get a prior (initial) solution by running the forward tidal model; run

fwd_fac -u1

5) compute the error covariance scales; run

diffuse

6) make the OTIS covariance file (../prm/covsc); run

varest

7) compute the representers; run

repx

8) make the altimetry data set; run

makedat

9) make the "reduced" altimetry data set for assimilation and then add the IHO data set for assimilation; run

makeB

makeB -a -D../prm/iho_data.dat -t

10) make the spatial representer matrices; run

rpx_to_p

rpx_to_p -r

11) calculate the representer coefficients; run

reduce_b

12) run the tidal data assimilation model; run

rlc

13) inspect the OTIS output and compute mean and rms errors with respect to the tidal data at the IHO stations; run

/bin/otis_comp_iho_eas.x

4. EVALUATION OF COMPUTED TIDES/ EVALUATION GRID

The procedure used for evaluating the tidal solutions is to compare the tidal-constituent amplitude and phase computed using OTIS against the values from the IHO stations. As already noted, there are potential problems with such a comparison. The tides at some IHO stations may not be representative of the tide in the adjacent open ocean (i.e., the ocean resolved by the computed tidal solution). However, in spite of this, comparison of the computed tides with the IHO stations is probably the best evaluation that can currently be made.

Comparison of a computed tidal solution with unsuitable IHO stations can be reduced somewhat by restricting the comparison to IHO stations that lie within a certain distance of the nearest sea point of the computational grid. A number of comparisons were made to determine how much the error of the tidal solution changes as the maximum allowable distance between the IHO station and the nearest sea point of the grid is changed. Calculation of tidal errors in several different regions with different maximum allowed distances between the IHO station and the nearest sea point of the computational grid consistently indicated that, as the maximum distance was reduced from 50 km to about 10 km, the rms errors steadily decreased. Reducing the maximum allowable distance beyond about 10 km did not usually make much difference. Hence, the tidal error statistics were computed using a maximum allowable distance of 10 km.

Since OTIS assimilates tidal data from IHO stations, one might question the validity of evaluating the resulting tidal solutions against the same IHO stations. However, since OTIS computes a single, continuous tidal solution over the domain on which it is run that is consistent with the dynamics imposed by the tidal equations, it cannot draw to every data value being assimilated. OTIS will try to minimize the overall error of the fit to the assimilated data of a consistent tidal solution. Hence, computing the error of the tidal solution with respect to the IHO stations is still a useful measure of the error of the solution.

When comparing the tidal solution computed on a particular grid with the IHO stations, there is the choice of whether to do the comparison on the computational grid that was used, which will vary if we are considering different grid resolutions or different sources of bathymetry, or to interpolate to a common grid. There are pros and cons for both choices.

Comparison on the original computational grid has the advantage that the maximum number of IHO stations are compared to the model sea points. However, some unsuitable IHO stations will

still be included depending upon how the computational grid coincides with the true coastline. A disadvantage of doing the comparisons on the computational grid (the resolution or bathymetry are changed) is that different computational grids will result in some different IHO stations being involved in the comparison, which will lend a bit of arbitrariness to the error calculations, i.e., including different IHO stations in the error statistics will generally change the computed error.

We used a standardized $1/12^\circ$ by $1/12^\circ$ evaluation grid to compare the OTIS results with the data from IHO stations within the EAS domain. The tidal solution was interpolated from the computational grid to the standardized evaluation grid and then the error statistics were computed. The main questions regarding setting up such a tidal evaluation grid are: (1) what grid resolution to use, and (2) how to define the land and sea areas.

Since a range of grid resolutions may be used for the tidal calculations, the evaluation grid should be at least the highest resolution used for the model run so the solutions do not lose accuracy. The land-sea areas are defined in the evaluation grid to incorporate as many IHO stations as were used in the experimental run.

The procedure used to spatially interpolate the tides is: (1) convert the tidal constituents from amplitude and phase to complex amplitude form, (2) do a horizontal "fill" of the complex amplitude values from the sea points out over the land points of the original (computational) grid (this is to allow interpolation to the sea points on the new grid that are not surrounded by sea points on the original grid), (3) interpolate the complex amplitudes for each tidal constituent to the new (evaluation) grid using bi-linear interpolation, and (4) if amplitude and phase information are desired, compute this from the complex amplitude on the new grid.

It is more accurate to spatially interpolate tidal harmonics fields in complex amplitude form rather than in amplitude and phase form. Hence, the tidal harmonic data in the TDBs are usually stored in complex amplitude form to be easily interpolated to a specified location. This same logic is used to spatially interpolate vector fields in vector form, rather than in magnitude and direction form.

5. SETTING UP A TIDAL COMPUTATION GRID

Bathymetry is important for all aspects of ocean circulation, but is especially important for the tides. There are other factors involved in the behavior of the tides in the ocean, but the most important factor governing the propagation of the tides is bathymetry.

Since bathymetry is so important, NRL has invested a fair amount of effort into developing good oceanic bathymetry databases. The main bathymetric database that we use is referred to as NRL's DBDB2, with the "2" referring to the database's 2-minute ($1/30^\circ$) resolution. New and improved bathymetry data that become available from both internal and external sources are incorporated into DBDB2 as soon as time and resources permit. In turn, DBDB2 has been made available to the oceanographic community at large.

For grid resolutions coarser than 2 minutes (about 2 to 3.7 km at low and mid latitudes), DBDB2 provides our best currently-available bathymetry. For higher-resolution grids, other bathymetry sources need to be considered. The National Oceanic and Atmospheric Administration (NOAA) has made available high-resolution (up to 3-second) gridded bathymetries for U.S.

coastal areas (http://www.ngdc.noaa.gov/mgg/bathymetry/hydro.html). High-resolution grids can be generated using sounding data in conjunction with the high-resolution World Vector Shoreline (WVS), assuming sufficient sounding data are available. We have recently begun collecting sounding data for the purpose of improving our gridded bathymetries and for generating more-highly-resolved model grids.

Something to be kept in mind when using bathymetric data is that, for navigational purposes, it is usually referenced to low tide (or tidal stage). Since our ocean models (including tidal models) are generally referenced to the mean SSH, the bathymetries we use need to be corrected for their reference to low tide. This can be done using a TDB to add to the bathymetry values the depth due to the amplitude of the local low tide.

Another consideration in setting up a computational grid is where to define the coastline. In models that do not provide for wetting and drying, a minimum depth at sea points needs to be prescribed to keep grid cells from drying out (note, however, that a minimum depth is not required for running OTIS).

6. CALCULATION OF TIDES IN THE YELLOW SEA WITH OTIS

The YS has some interesting tides (e.g., the very large tides along parts of Korea's west coast), has been the subject of a number of tidal studies (e.g., Teague et al., 2000 and 2006), and hence, provides a useful testbed for OTIS. The YS is large enough to have a varied and distinctive tidal structure, but is sufficiently small that OTIS runs can be performed fairly quickly. This is a significant advantage over running OTIS for the entire EAS domain, which requires much more computer time. The standard grid used for the YS is 33 to 41°N and 117 to 127°E with a spatial resolution of approximately 1/12° and grid dimensions of 120 x 96. An OTIS run for the YS on this grid takes less than 10 minutes on our standard LINUX platforms.

Figure 3 illustrates how different two bathymetry datasets for the Yellow Sea region can be. The left side shows the ETOPO5 5-minute bathymetry (this database was included with the OTIS software from OSU) interpolalated to a grid with (the same) 1/12° resolution, while the right side shows NRL's DBDB2 2-minute bathymetry interpolated to a grid with 1/24° resolution. The differences are quite large.

Figure 4 provides a comparison of the M2 tidal amplitude from two OTIS runs with a maximum contrast in run conditions. The left side of the figure shows a YS OTIS run with ETOPO5 bathymetry, 1/12° grid resolution, and use of the OSU global TDB for TBCs. The right side of the figure shows a YS OTIS run with DBDB2 bathymetry, 1/24° grid resolution, and the OSU YS TDB for TBCs (this is our benchmark run for the Yellow Sea). The RMS error between the OTIS tidal solutions and the IHO data (within the 10-km distance limit) was 0.729 m for the case on the left and 0.129 m for the case on the right. Both visually (i.e., compared with previous tidal solutions in the YS) and as indicated by the computed errors, the OTIS solution with the better DBDB2 bathymetry and higher grid resolution is greatly improved.

We performed a number of comparison tests in the YS area, varying several parameters within the default OTIS parameter list. Table 2 provides a summary of the parameters that were tested. These include varying the bathymetry, the OBCs, and the grid resolution, using variable instead of

constant bottom friction, using computed normalization scales for the error covariance, and using a nonlinear instead of a linear a priori solution.

One of the major changes was to the truncation parameter, which sets a limit on the number of representer matrix modes to be used in the model solution. The default truncation was originally set to 50, which allowed only the top 50 most influential representer matrix modes to be used in the model solution. We found that, if we increased this number, the final solution improved significantly. A direct result of this testing was the development of software to calculate an optimum truncation value based on available computer resources.

During our sensitivity studies of the YS area, we compared our benchmark OTIS solution (with the DBDB2 bathymetry, BC from the OSU YS TDB, 1/24° grid resolution, and the 4 major tidal constituents) to the IHO tide-gauge measurements to estimate the error for different regions of the YS. Figure 5 shows four areas of interest: Area A - Incheon Bay, Area B - Kored Bay, Area C - the Liautung Gulf, and Area D - Bo Hai Bay.

Figure 6 shows the mean M2 amplitude error of the OTIS solution relative to the IHO stations for Incheon Bay. A negative value indicates that the OTIS solution underestimates the amplitude. Figure 7 shows the mean M2 amplitude error for Kored Bay, Fig. 8 for the Liautung Gulf, and Fig. 9 for Bo Hai Bay. In all four of these areas, the OTIS solution underestimates the M2 tidal amplitude. For Incheon Bay, Kored Bay, the Liautung Gulf, and Bo Hai Bay, the RMS errors for the M2 amplitude are -0.44 m, -0.04 m, -0.10 m, and -0.06 m, respectively.

6.1 OTIS results compared with independent Korean Strait data

The Korea/Tsushima Strait lies between the Republic of Korea and Fukuoka, Japan, and is a shallow area with depths of about 100 m. A set of measurements from this region was used for an OTIS validation. Figure 10 shows the positions of 11 bottom-mounted ADCPs deployed for 11 months during 1999-2000 as part of NRL's Dynamical Linkage of Asian Marginal Seas (LINKS) program (Teague et al., 2000). The moorings were divided into two lines, the northern line on the Sea of Japan side of the strait and the southern line on the East China Sea/Yellow Sea side of the strait. The OTIS model results compared very well against the LINKS dataset. The RMS amplitude error for the four major tidal constituents (M2, S2, K1, and O1) ranged from 1 to 5 cm. The RMS phase error for the major tidal constituents ranged from 6 to 59 degrees. See Table 3 for comparisons of the individual constituents.

7. CALCULATION OF TIDES IN THE EAS WITH OTIS

Several sensitivity studies were conducted in the EAS region during our OTIS evaluation. The tests included varying (1) the grid resolution, (2) the bathymetry, (3) the number of representers used for the data assimilation, and (4) the number of tidal constituents. All the test grids used the same beginning and ending longitude and latitude for the EAS region, i.e., -17.5 to 53.0°N and 97.5 to 159°E.

7.1 Higher grid resolution

The first set of tests for the EAS domain concerned varying the grid resolution. All of these tests used NRL's DBDB2 bathymetry and 4 tidal constituents (M2, S2, K1, and O1). The original

grid (which later became the benchmark grid for the EAS region) used a resolution of 0.08° in longitude and 0.14° in latitude and 700 x 507 gridpoints. This case took 26 hours to run.

For the second grid, the grid spacing was set to 0.10° in both longitude and latitude, which increased the grid dimensions to 615 x 705 and increased the runtime by 2 hours (from 26 to 28 hours). The results were worse in amplitude for M2 and K1, but slightly better for S2. (Table 4). The results were slightly better in phase than the standard grid results.

The third test consisted of increasing the grid resolution to 0.08° in both longitude and latitude, which increased the grid dimensions to 728 x 846. Because of the large grid, this case had to be run on a super-linux computing platform that had more memory than our standard computing platforms. The run time for this case was 61 hours. The results from this test were again worse in amplitude for M2, but slightly better in phase for M2 and slightly better in both amplitude and phase for S2, O1, and K1.

Since M2 is the most dominant constituent for the EAS area, it was decided to use the first grid (700 x 507) as the standard benchmark grid. Along with getting the best results in amplitude and phase for M2, the first grid ran the most quickly.

7.2 Better bathymetry

The second set of tests concerned varying the bathymetry. The original bathymetry provided with OTIS was ETOPO5, which is derived from a relatively old bathymetry with 5-minute (1/12°) resolution. OTIS has been updated to use NRL's DBDB2 2-minute (1/30°) bathymetry. A comparison of the ETOPO5 and DBDB2 bathymetries in the YS region of the EAS is shown in Fig. 3. The higher-resolution DBDB2 bathymetry (on the right side of the figure) looks more detailed than the ETOPO5 bathymetry (on the left side).

The OTIS run using the DBDB2 bathymetry has smaller RMS errors than the OTIS run using the ETOPO5 bathymetry for all four tidal constituents for both amplitude and phase (Table 5). The run times for both of these cases were the same at 26 hours.

7.3 Increasing the number of representers

The third set of tests concerned varying the number of representers (i.e., data-assimilation locations) used in the data assimilation scheme of OTIS. We had initially assumed that, if more representers were included in the simulation, the results should be better. Three studies were performed with the number of representers set to 1000, 2000, and 3000.

Increasing the number of representers from 500 to 1000, the RMS amplitude error decreased for all 4 constitutents, with only slight changes in the phase error. Increasing the number of representers from 1000 to 2000, the RMS amplitude and phase errors decreased for the M2 and S2 constituents, but increased slightly for K1 and O1 (Table 6). The RMS phase error increased slightly for all the constitutents except S2, and the run time increased from 31 to 37 hours.

Increasing the number of representers from 2000 to 3000 resulted in a small increase in the M2 phase error, but little or no changes in the other errors (Table 6). The run time with 3000

representers increased to 40 hours. Hence, there appeared to be no advantage to using 3000 representers for the EAS domain. The default value for the number of representers used in all the other tests was 500.

7.4 Inclusion of additional tidal constituents

The last set of tests concerned varying the number of tidal constituents used in the OTIS simulation. Like most of the other tests, the time required for the run increased as the number of constituents was increased. Using one constituent (M2), the runtime was 4 hours. The run time increased to 26 hours for 4 constituents and was 24 hours for 8 constituents. The decrease in runtime for the 8 constituent test is due to the fact that OTIS includes in the assimilation only stations that have all the constituents being used, and there are significantly fewer IHO stations that have all 8 main constituents (K1, O1, P1, Q1, K2, M2, N2, S2) than have the four main constituents (K1, O1, M2, S2). For example, for this set of tests, the tests with 1 and 4 tidal constitutents assimilated 630 and 628 stations, respectively, whereas, the test with 8 tidal constituents assimilated only 142 stations.

The results for this set of tests are listed in Table 7. Changing the number of constituents from 1 to 4 slightly increased the M2 RMS amplitude error from 0.104 to 0.114 m. The reason for the larger error is not currently understood since the number of stations assimilated for these two cases was almost the same. By changing the number of constituents from 4 to 8, the M2 amplitude error almost doubled from 0.114 m to 0.218 m. This larger error is due to the much smaller number of IHO stations being assimilated into the OTIS run. The errors in Table 7 are predominantly computed in coastal regions, since this is where the majority of IHO stations are located. Therefore, in the 8 constituent case, the decrease in the number of IHO stations being assimilated is causing a reduction in accuracy in the important coastal regions.

8. EFFECT OF NEW TDBS ON TIDES IN THE EAS MODEL

As noted earlier, NRL's EAS model was recently modified to include tides (Reidlinger et al., 2006). The TBCs for the EAS model were initially obtained (interpolated) from OSU's Global TDB. The EAS model was run with TBCs obtained from the TDBs generated in this study with OTIS to look at the effect of these new TBCs on the tides predicted by the EAS model. The tides simulated by the EAS model were evaluated by computing tidal errors with respect to the IHO stations.

Table 8 demonstates the large improvement in accuracy that using the inverse tidal solution can have in coastal regions compared to using relatively coarse, regional TDBs. The Yellow Sea inverse solution was computed using DBDB2 bathymetry, a 1/24° grid, and TBCs from a regional Yellow Sea TDB; whereas, the OSU global TDB has a resolutiong of 1/4°. The prediction of tides in coastal regions is significantly more complicated than in the open ocean. Therefore, it is clear that the inverse solution ought to be computed with a high-resolution bathymetry and grid in order to achieve sufficient accuracy in these types of regimes.

Another important contributor to the the improved accuracy of the Yellow Sea inverse solution over the global TDB is the use of localized data from the IHO database. By computing an inverse solution on a high-resolution grid for a localized marginal sea (such as the Yellow Sea), this solution

will rely more heavily on the IHO data and the data will be positioned more accurately on the high-resolution grid. As mentioned previously, inverse solutions are computed by assimilating both TOPEX altimetry and IHO tide-gauge data. However, the OSU global TDB was established using only TOPEX data, and TOPEX data are less accurate in shallow waters.

Note that since (a) the OSU TDBs are fairly good in the open ocean away from the coasts and (b) most of the open boundaries of the EAS model domain are in the open ocean, it was not expected that improvement of the TDBs generated with OTIS within the EAS region (where the improvement is mainly in the coastal areas) would have a large effect on the tides simulated by the EAS model. The improved TDBs should have a more significant effect on the tidal simulation within smaller, coastal domains (as illustrated for the YS in Section 6).

The tides simulated by the EAS model were tested by running with one tidal constituent at a time. This was done to reduce the computer time required to perform the tests, since a long model run (typically six months) is needed to allow a tidal analysis to separate tidal constituents with frequencies that only differ by only a small amount, e.g., M2 and S2 or K1 and O1. A model simulation with a single tidal constituent need only be run for a few days to allow fairly accurate calculation of the predicted amplitude and phase of the constituent over the model domain.

Two types of simulations were run to look at the tides simulated by the EAS model. In the first type, the EAS model was run as a single-layer, homogeneous (constant density) model with only tidal forcing. In the second type, the EAS model was run in its full baroclinic form as it is normally run at NRL (Reidlinger et al., 2006), i.e., with 40 vertical layers and variable temperature and salinity, initialization of all predicted fields (SSH, velocity, temperature, and salinity) from NRL's EAS model for 30 December 2005, real-time (non-tidal) boundary conditions from NRL's global NCOM model, atmospheric forcing from the Navy Operational Global Atmospheric Forecast System (NOGAPS), and monthly climatological river inflows from NRL's global river database. Both types of simulations used the same horizontal grid, bathymetry, and coastline. For the tests conducted here, the EAS model was run for 12 days and a tidal analysis of the model-predicted SSH was performed over the last 10 days of the run.

Table 9 lists the RMS errors for the tidal amplitude and phase for the SSH predicted by the EAS model for the full baroclinic run for TBCs obtained from (a) the OSU Global TDB and (b) the OTIS benchmark run (on the 700 x 507 grid) described in the previous section. The errors were computed with respect to about 1200 IHO stations located within the EAS domain for the four main tidal constituents (M2, S2, K1, and O1). As in previous error calculations, only IHO stations within 10 km of a sea point of the EAS model grid were used to compute the errors.

The differences in the errors for the OSU Global and OTIS TBCs in Table 9 are small, i.e., there is a slight improvement in the RMS error for M2, K1, and O1 but these improvements are too small to be significant. As noted earlier, this was not unexpected, since most of the open boundaries of the EAS domain are in the open ocean where all the OTIS solutions are strongly constrained by the satellite data.

9. SUMMARY, CONCLUSIONS, AND FUTURE WORK

The Naval Research Laboratory (NRL) has been testing and developing ocean tidal solutions using the Oregon State University (OSU) Tidal Inversion Software (OTIS). OTIS has been applied

to several areas including the East-Asian Seas (EAS) and the Yellow Sea (YS). The major testing of parameters has been performed in the YS due to is small size and small computer requirements. Tests were conducted to look at the effects on the OTIS results from changes in a number of inputs including: (1) increasing the grid resolution, (2) using more accurate bathymetry, (3) assimilating IHO tide station data in addition to tidal data derived from TOPEX altimeter data, (4) increasing the number of representers used for data assimilation, and (5) increasing the number of tidal constituents. Work is also ongoing to generalize the configuration of and automate the overall system.

The effects of the above listed changes to the OTIS inputs were much more significant in the tests conducted in the YS than those conducted in the larger EAS domain. The OTIS tidal solutions in the YS were greatly improved by increasing the grid resolution, using more accurate bathymetry, and assimilating IHO data. For the OTIS tidal solutions in the EAS region, the most significant improvement came from improving the bathymetry. The particular increases in the grid resolution and the number of representers for the EAS region that were tested had only a small effect on the tidal errors.

Further work needs to be done to develop a fuller understanding of the effects of changes in the inputs to the OTIS runs on the OTIS tidal solutions. Future work will also include testing OTIS (and the changes being made to OTIS) in additional littoral regions. During our Validation Test Panel (VTP) meeting held Sept 2008, NAVOCEANO suggested the following areas for additional testing: the East China Sea, the South China Sea, the Persian Gulf, the US East Coast (Cuba to Delaware Bay), and the US west coast (Montery Bay).

10. ACKNOWLEDGMENTS

This work was sponsored by the Space and Naval Warfare Systems Command under the Small-Scale-Prediction Program (Program Element 0603207N). Additional thanks goes to Gary Egbert and Lana Erofeeva at Oregon State University for providing the initial software package and their guidance regarding its operation.

11. REFERENCES

Egbert, G., Bennett, A. and Foreman, M. (1994). TOPEX/POSEIDON tides estimated using a global inverse model. *J. Geophys. Res.*, *99(C12)*, 24,821–24,852.

Egbert, G., (1997). Tidal data inversion: interpolation and inference. *Prog. Oceanog. 40*, 53–80.

Egbert, G., and Ray, R., (2001). Estimates of M2 tidal energy dissipation from TOPEX-POSEIDON altimeter data. *J. Geophys. Res.*, *106(C10)*, 22,475–22,502.

Egbert, G., and Erofeeva, S. (2002). Efficient inverse modeling of barotropic ocean tides. *J. Atmos. Oceanic Technol.*, *19*, 183–204.

Egbert, G., and Ray, R., (2003). Semi-diurnal and diurnal tidal dissipation from TOPEX-POSEIDON altimetry. *Geo. Res. Let.*, *30(17)*.

Erofeeva, S., Egbert, G., and Kosro, P., (2003). Tidal currents on the central Oregon shelf: Models, data and assimilation. *J. Geophy. Res.*, *108(C5)*, 3148.

Martin, P.J., J.W. Book, and Doyle, J.D., (2006). Simulation of the northern Adriatic circulation during winter 2003. *J. Geophy. Res.*, *112(C3)*, C03S12.

Pond, S. and Pickard, G. (1989). *Introductory Dynamical Oceanography*, Second Edition, Pergamon Press, pp. 329.

Riedlinger, S., Preller, R. and Martin, P., (2006). Validation test report for the 1/16 degree East Asian Seas navy coastal model nowcast/ forecast system. NRL/MR/7320–06-8978.

Teague, W., Pistek, P., Jacobs, G., Perkin, H., (2000). Evaluation of tides from TOPEX/POSEIDON in the Bohai and Yellow Seas. *J. Atmos. Oceanic Technol.*, *(17)*, 679–687.

Teague, W., Pistek, P., Jacobs, G., Perkin, H., (2006). Currents through the Korea/Tsushima Strait: A review of LINKS observations. *Oceanography*, *19(3)*, 50–63.

Webb, D., (1974). Green's function and tidal prediction. *Review of Geophysics and Space Physics*, *(12)*, 103–116.

http://www7320.nrlssc.navy.mil/DBDB2_WWW/

http://www.ngdc.noaa.gov/mgg/bathymetry/hydro.html/

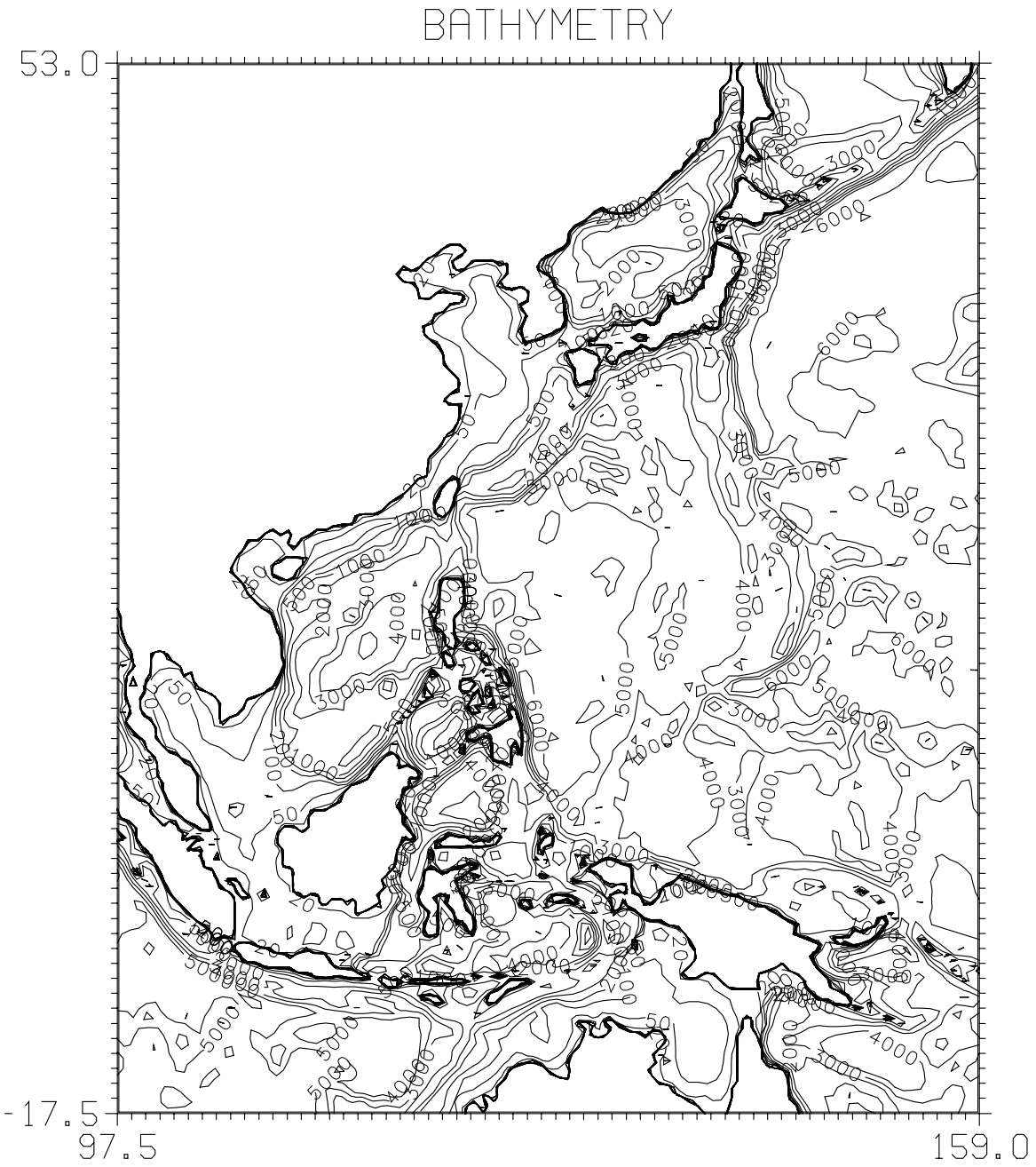

Fig. 1 — Domain and bathymetry (m) for EAS.

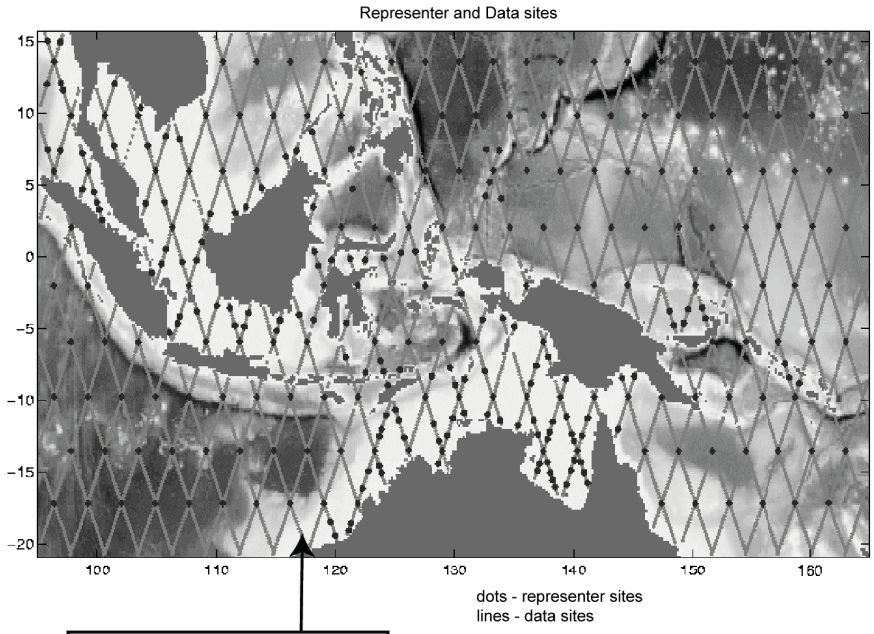

Regional Indonesian Seas OTIS solution

Global OTIS solution that is used within EAS NCOM

RMS Errors

	Depth range	Inverse	Prior	TPXO.3	GOT99	CSR4.0	HC errors
M_2	H<500m	3.8	11.4	11.2	5.8	9.5	1.6
	500m<H<2500m	1.9	9.2	6.1	2.8	3.8	1.1
	2500m<H<4000m	1.4	7.1	3.6	1.5	2.2	1.1
	H>4000m	1.3	5.6	2.3	1.3	1.5	1.0
S_2	H<500m	2.5	9.2	7.8	3.7	5.6	1.7
	500m<H<2500m	1.3	7.3	3.8	2.0	2.4	1.1
	2500m<H<4000m	1.0	5.7	2.5	1.1	1.4	1.1
	H>4000m	0.9	4.3	2.0	1.0	1.0	1.0
K_1	H<500m	2.7	10.5	6.7	4.6	7.3	1.8
	500m<H<2500m	1.6	5.2	2.1	2.0	2.7	1.2
	2500m<H<4000m	1.3	3.7	1.5	1.4	1.9	1.2
	H>4000m	1.3	2.8	1.3	1.3	1.5	1.1
O_1	H<500m	2.2	8.1	5.1	2.7	3.4	1.9
	500m<H<2500m	1.1	3.6	1.5	1.3	1.9	1.3
	2500m<H<4000m	0.9	2.6	1.1	1.0	1.3	1.3
	H>4000m	0.9	1.9	1.1	0.9	1.0	1.2

Fig. 2 — RMS Comparison for the Indonesian Seas regions (G. Egbert and S. Erofeeva, 2002).

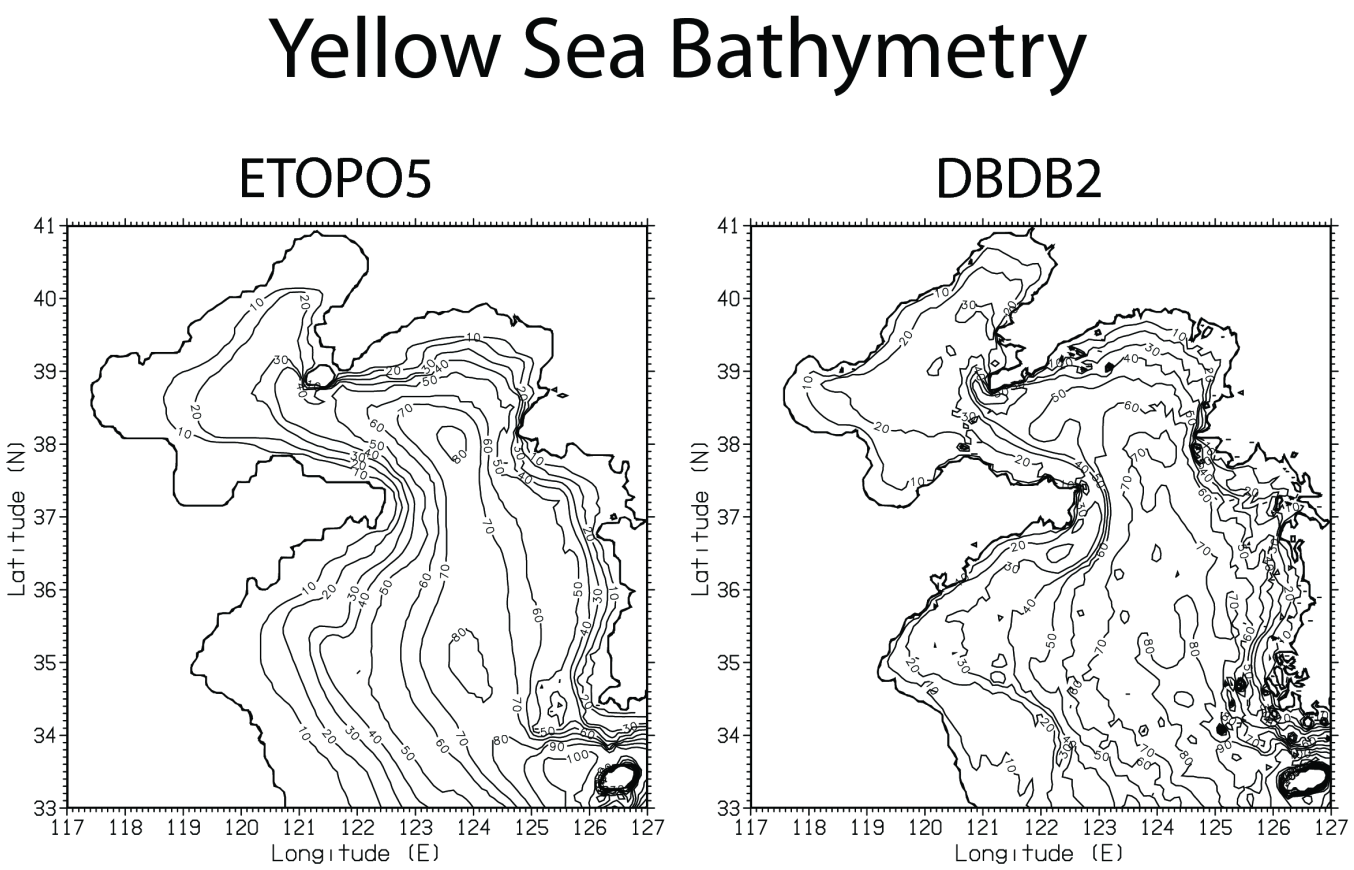

Fig. 3 — Comparison of ETOPO5 and DBDB2 bathymetries in Yellow Sea.

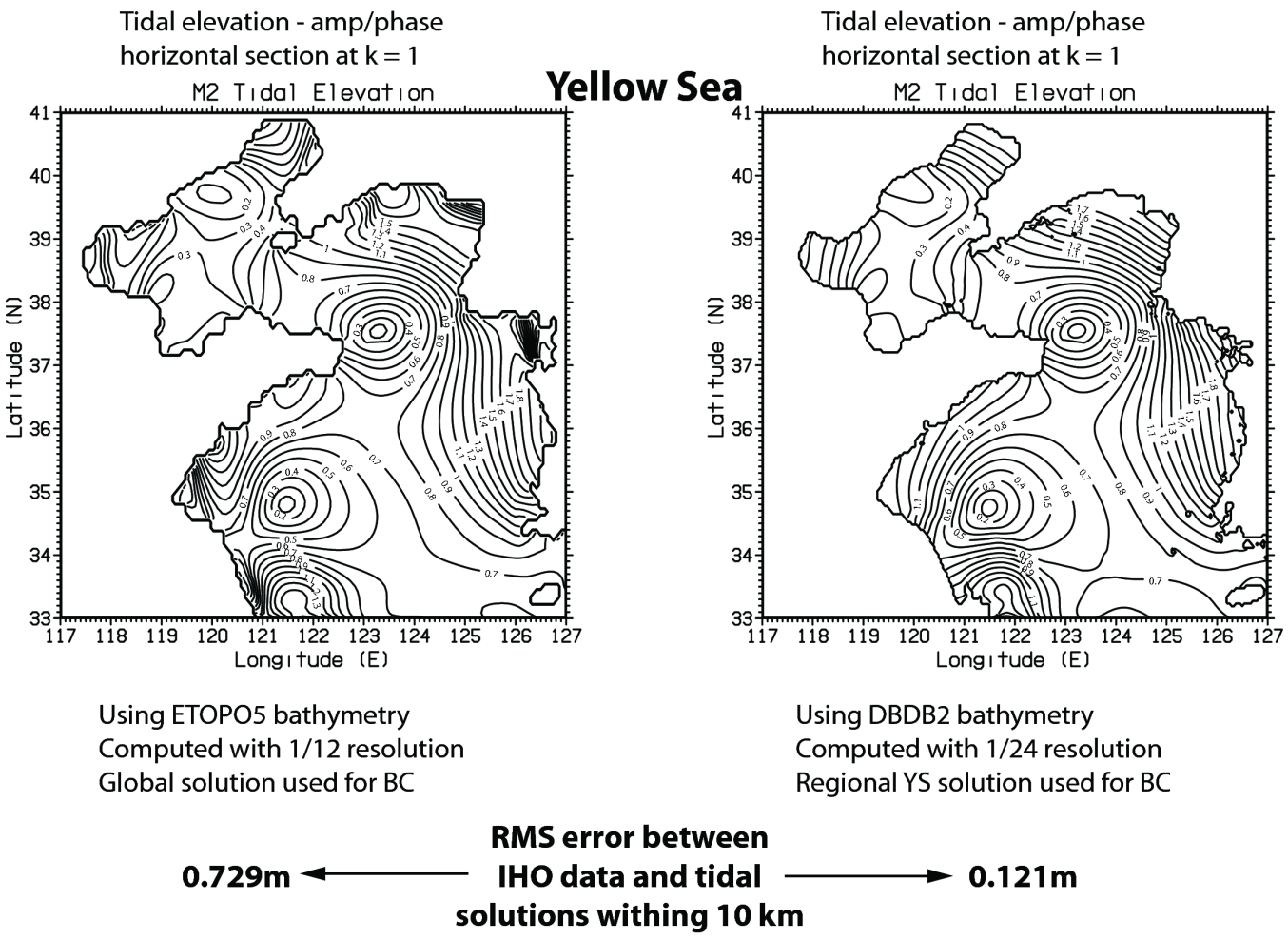

Fig. 4 — Comparison of M2 tidal amplitude (m) in Yellow Sea.

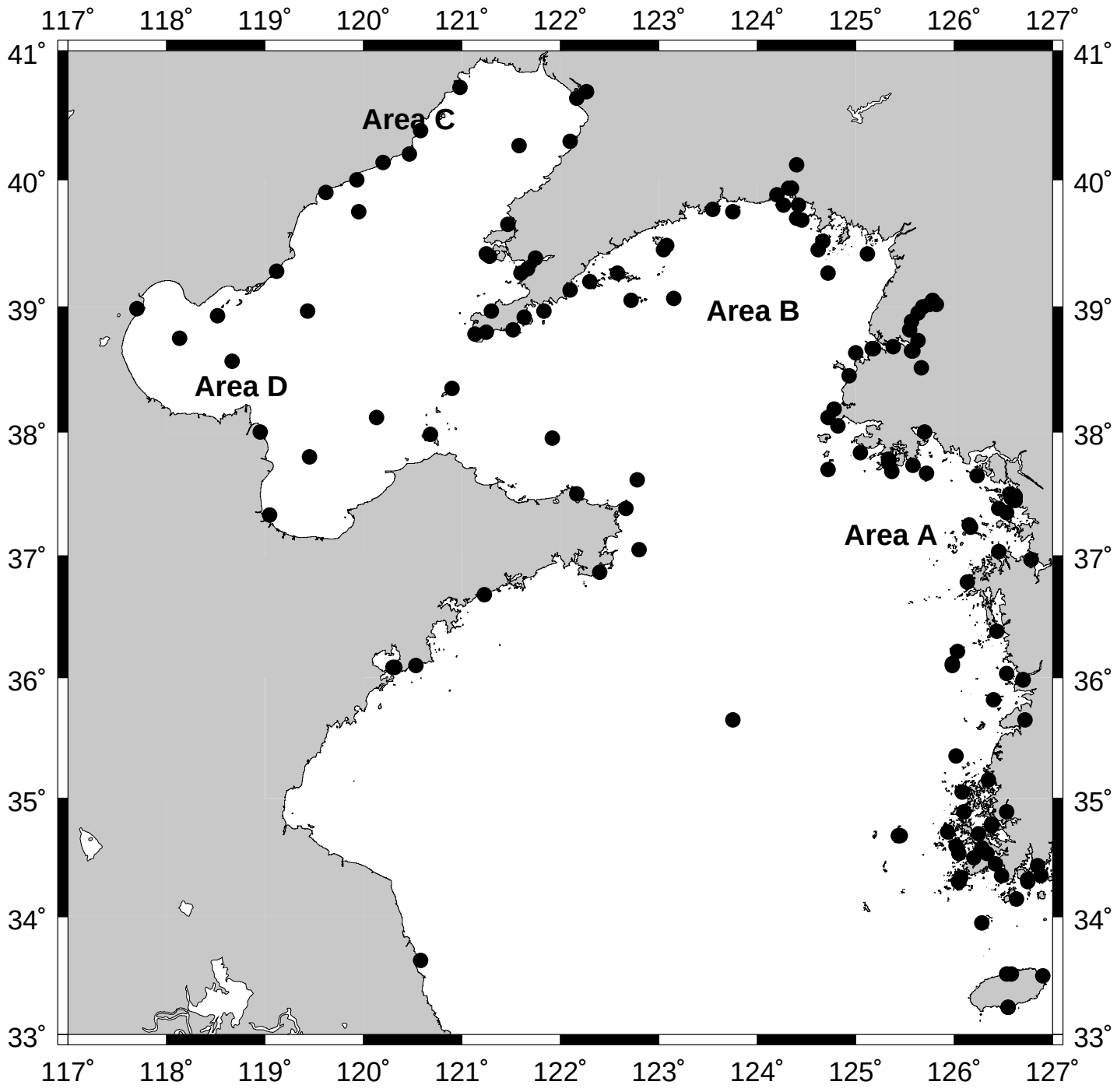

Fig. 5 — Four areas of interest in the Yellow Sea (Area A - Incheon Bay, Area B - Kored Bay, Area C - Liautung Gulf and Area D - Bo Hai Bay.

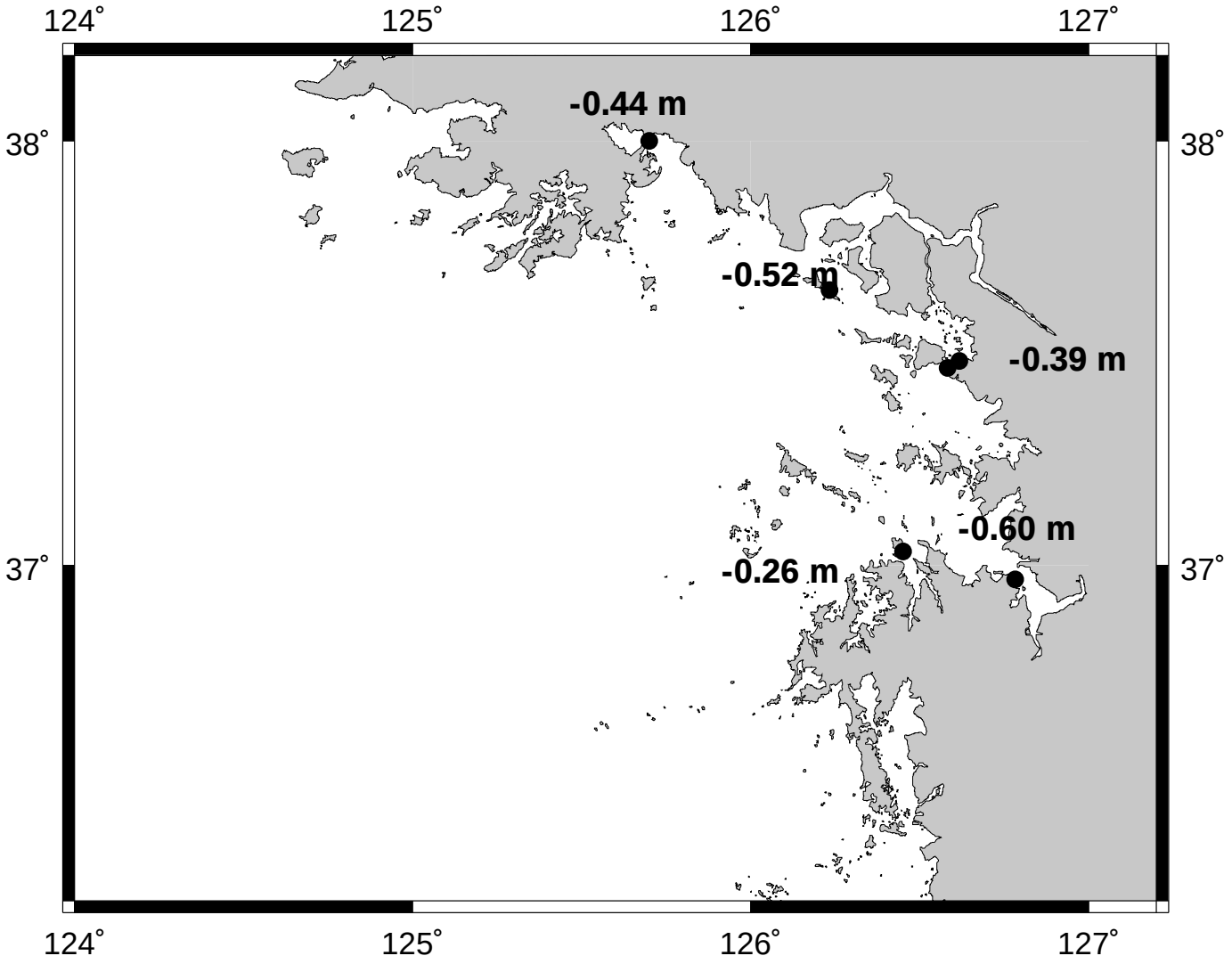

Fig. 6 — Mean M2 amplitude error for Incheon Bay stations.

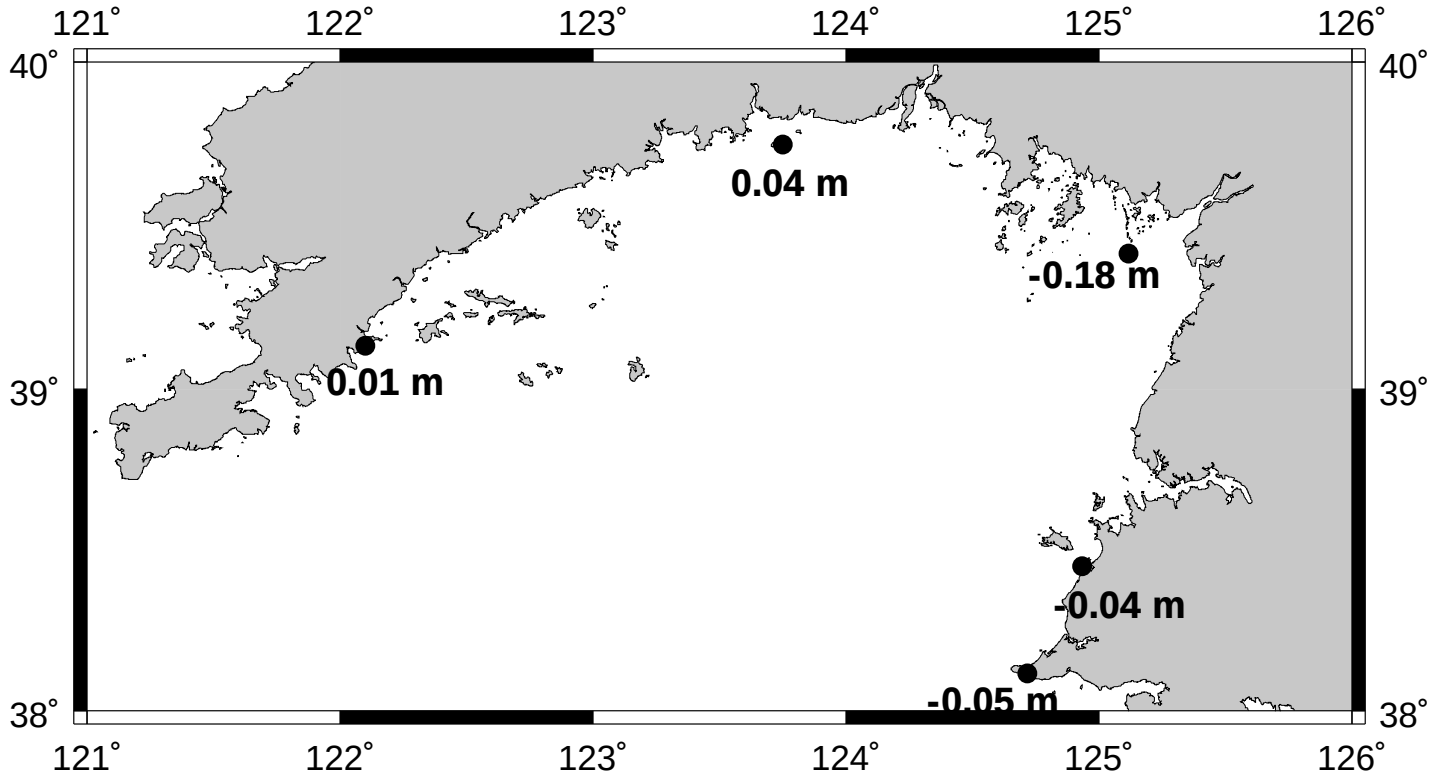

Fig. 7 — Mean M2 amplitude error for Kored Bay stations.

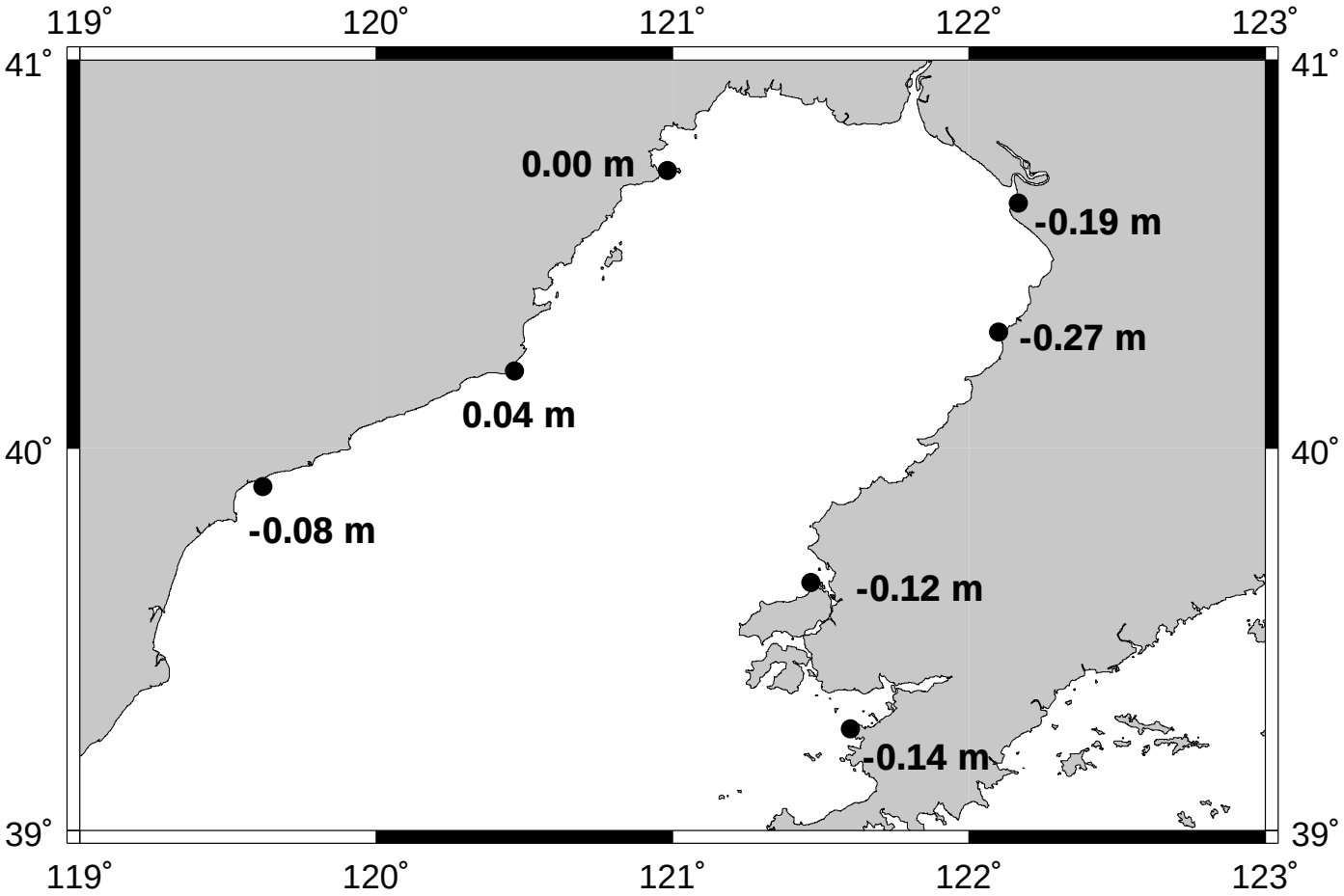

Fig. 8 — Mean M2 amplitude error for Liautung Gulf stations.

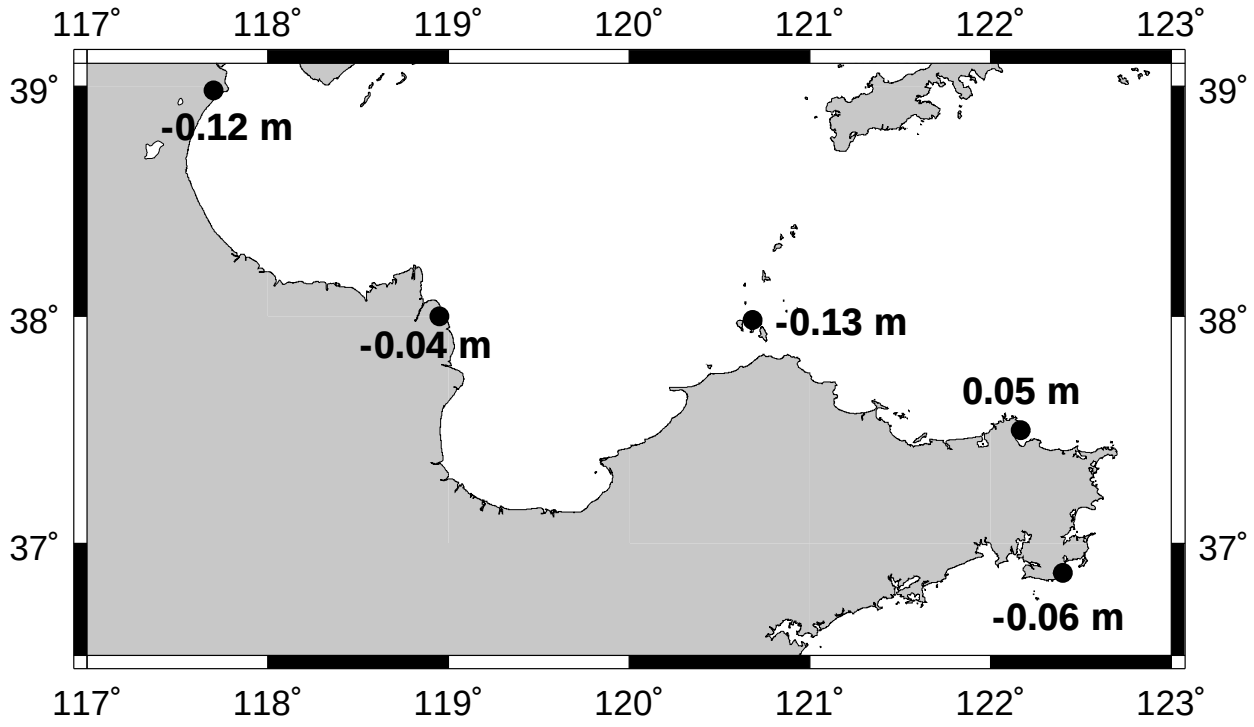

Fig. 9 — Mean M2 amplitude error for Bo Hai Bay stations.

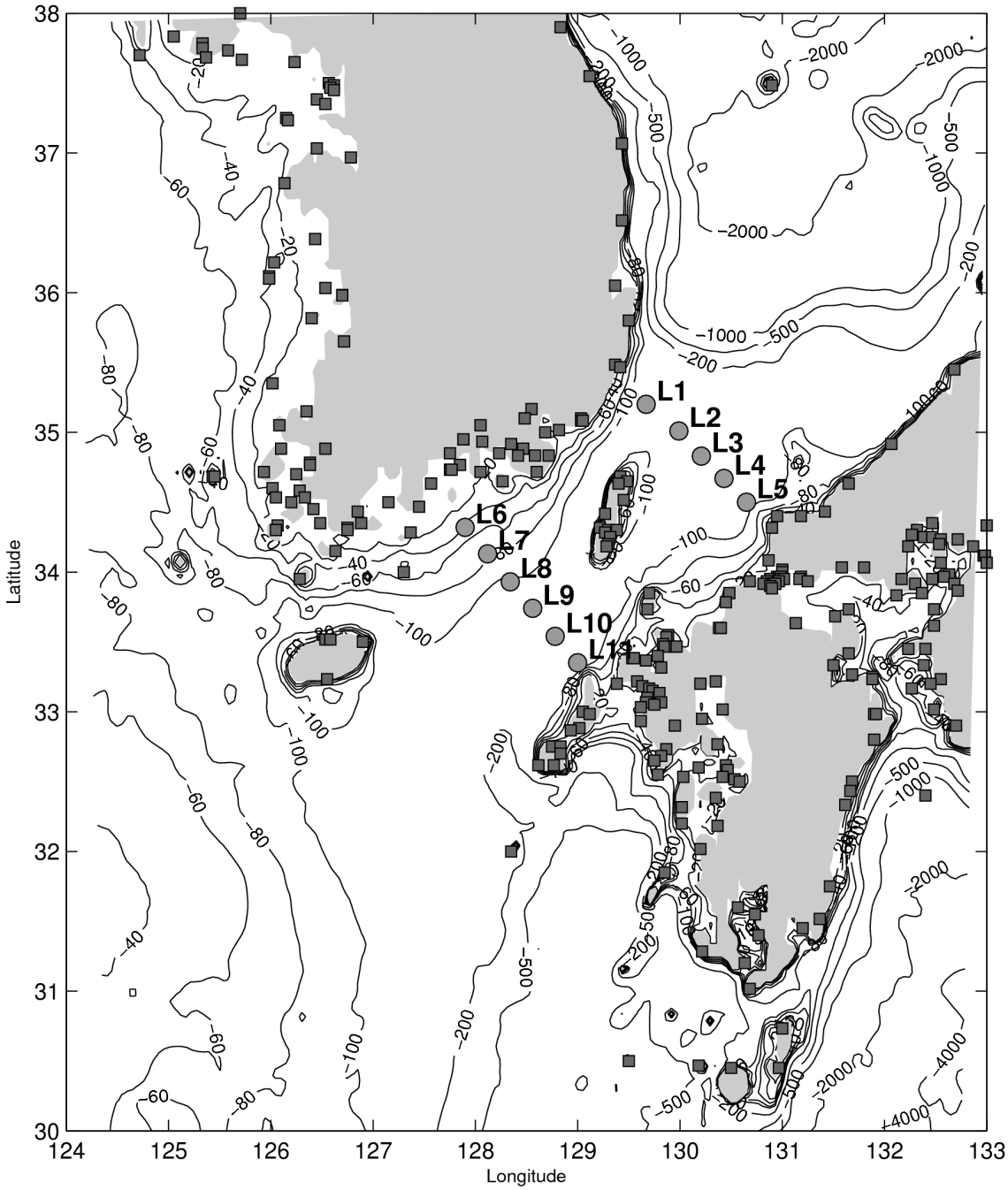

Fig. 10 — Bathymetry (m) of the Korean Strait. Squares indicate the IHO staions and circles indicate the location of bottom-mounted ADCPs.

Table 1 — OTIS tidal databases from OSU

database	resolution	no. of constituents	region
Global	1/4°	10	global
Indonesia	1/6°	8	95 to 165E,-21 to 15.6667N
Mediterranean	1/12°	4	-5.583 to 36.333E, 30.416 to 45.916N
North Atlantic	1/12°	8	-100 to 15E, -5 to 75N
US West Coast	1/12°	8	225.0 to 255.0E, 21 to 50N
Yellow Sea	1/12°	4	105.25 to 129.25E, 14 to 42N
Hudson Bay	1/12°		
U.S.West Coast	1/12°		
Arabian Sea	1/12°		
Bering Sea	1/12°		
North Sea	1/12°		
Gulf of Mexico	1/12°		
Bay of Bengal	1/12°		
Tasmania	1/30°		
Hawaii	1/30°		
Oregon	1 km		
Arctic	5 km		

Table 2 — Summary of sensitivities studies for the Yellow Sea

Bathymetry	OBC from	Res.	Min depth	Const friction	Error	Comp. time
ETOPO5	Global	1/12°	10 m	1 m/s	0.729 m	3 min
DBDB2	Global	1/12°	10 m	1 m/s	0.164 m	3 min
DBDB2	Regional YS	1/12°	10 m	1 m/s	0.158 m	3 min
DBDB2	Regional YS	1/12°	5 m	1 m/s	0.300 m	3 min
DBDB2	Regional YS	1/12°	1 m	1 m/s	0.391 m	3 min
DBDB2	Regional YS	1/24°	10 m	1 m/s	0.129 m	5 min
DBDB2	Regional YS	1/12°	10 m	0.5 m/s	0.218 m	3 min
DBDB2	Regional YS	1/12°	10 m	2 m/s	0.218 m	3 min
DBDB2	Regional YS	1/12°	10 m	3 m/s	0.232 m	3 min
DBDB2	Regional YS	1/12°	10 m	4 m/s	0.221 m	3 min
DBDB2	Regional YS	1/12°	10 m	5 m/s	0.206 m	3 min
Computed variable bottom friction					0.249 m	3 min
Computed nonlinear a priori solution					0.135 m	19 min
Computed normalization scales for error covariance					0.152 m	3 min
Computed both variable bottom friction and normalization scales					0.245 m	3 min

Table 3 — OTIS results compared against independent Korean Strait data

	rms error	
Constituent	amp(m)	phase(deg)
M2	0.052	5.9
S2	0.014	7.4
O1	0.014	58.7
K1	0.017	37.5

Table 4 — Varying Grid Resolutions for EAS region

	grid dimensions (deg)					
	0.08 x 0.14		0.10 x 0.10		0.08 x 0.08	
	rms error					
Constituent	amp(m)	phase(deg)	amp(m)	phase(deg)	amp(m)	phase(deg)
M2	0.114	27.6	0.133	27.6	0.129	26.0
S2	0.060	29.7	0.059	29.0	0.056	28.7
O1	0.044	19.2	0.044	17.3	0.044	17.5
K1	0.055	18.3	0.057	17.5	0.055	17.7

Table 5 — Varying source of bathymetry data for EAS region

	bathymetry			
	ETOPO5		DBDB2	
	rms error			
Constituent	amp(m)	phase(deg)	amp(m)	phase(deg)
M2	0.136	29.3	0.114	27.6
S2	0.063	32.3	0.060	29.7
O1	0.049	20.4	0.044	19.2
K1	0.068	20.0	0.054	18.3

Table 6 — Varying number of representers for data assimilation

	number of representers							
	500		1000		2000		3000	
	rms error							
Constituent	amp(m)	phase(deg)	amp(m)	phase(deg)	amp(m)	phase(deg)	amp(m)	phase(deg)
M2	0.114	27.6	0.107	27.7	0.103	29.3	0.102	28.9
S2	0.060	29.7	0.056	29.8	0.051	29.6	0.053	29.8
O1	0.044	19.2	0.041	18.9	0.042	19.2	0.042	19.3
K1	0.055	18.3	0.052	18.2	0.054	18.5	0.055	18.8

Table 7 — Varying number of tidal consitutents for EAS region

	number of tidal constituents					
	1		4		8	
	rms error					
Constituent	amp(m)	phase(deg)	amp(m)	phase(deg)	amp(m)	phase(deg)
M2	0.104	27.4	0.114	27.6	0.218	37.1
S2			0.060	29.7	0.163	35.8
O1			0.044	19.2	0.057	22.0
K1			0.055	18.3	0.081	24.4

Table 8 — Yellow Sea M2 RMS Error between IHO tide gauges and tidal solutions within 10 km

	Amp(m)	Phase (deg)
OSU Global Tidal Data Base	0.734	36.4
Yellow Sea Inverse Solution	0.121	26.3

Table 9 — Varying tidal boundary conditions for EAS model

	source of tidal boundary conditions			
	OSU Global DB		benchmark OTIS run	
	rms error			
Constituent	amp(m)	phase(deg)	amp(m)	phase(deg)
M2	0.248	33.6	0.247	32.2
S2	0.109	34.5	0.109	34.6
K1	0.086	23.0	0.083	22.7
O1	0.065	28.9	0.054	24.0